metals

Article

Effect of Milling Time and the Consolidation Process on the Properties of Al Matrix Composites Reinforced with Fe-Based Glassy Particles

Özge Balcı [1,2], Konda Gokuldoss Prashanth [2,†,*], Sergio Scudino [2], Duygu Ağaoğulları [1], İsmail Duman [1], M. Lütfi Öveçoğlu [1], Volker Uhlenwinkel [3] and Jürgen Eckert [2,4]

[1] Particulate Materials Laboratories (PML), Department of Metallurgical and Materials Engineering, İstanbul Technical University, 34469 İstanbul, Turkey; E-Mails: balciozg@itu.edu.tr (O.B.); bozkurtdu@itu.edu.tr (D.A.); iduman@itu.edu.tr (I.D.); ovecoglu@itu.edu.tr (M.L.O.)

[2] Institute for Complex Materials, IFW Dresden, 270116 Dresden, Germany; E-Mails: s.scudino@ifw-dresden.de (S.S.); j.eckert@ifw-dresden.de (J.E.)

[3] Institut für Werkstofftechnik, Universität Bremen, D-28359 Bremen, Germany; E-Mail: uhl@iwt.uni-bremen.de

[4] TU Dresden, Institut für Werkstoffwissenschaft, D-01062 Dresden, Germany

[†] Present Address: R&D Engineer, Additive manufacturing Center, Sandvik AB, 81181 Sandviken, Sweden; E-Mail: prashanth.konda_gokuldoss@sandvik.com.

[*] Author to whom correspondence should be addressed; E-Mail: kgprashanth@gmail.com; Tel.: +46-7277-91612; Fax: +46-2626-6125.

Abstract: Al matrix composites reinforced with 40 vol% $Fe_{50.1}Co_{35.1}Nb_{7.7}B_{4.3}Si_{2.8}$ glassy particles have been produced by powder metallurgy, and their microstructure and mechanical properties have been investigated in detail. Different processing routes (hot pressing and hot extrusion) are used in order to consolidate the composite powders. The homogeneous distribution of the glassy reinforcement in the Al matrix and the decrease of the particle size are obtained through ball milling. This has a positive effect on the hardness and strength of the composites. Mechanical tests show that the hardness of the hot pressed samples increases from 51–155 HV, and the strength rises from 220–630 MPa by extending the milling time from 1–50 h. The use of hot extrusion after hot pressing reduces

both the strength and hardness of the composites: however, it enhances the plastic deformation significantly.

Keywords: metallic glasses; composites; powder metallurgy; mechanical characterization

1. Introduction

Al-based metal matrix composites (MMCs) have attracted considerable interest due to their superior properties, including high strength and good fatigue and wear resistance [1–3]. They are advanced engineering materials able to meet the increasing demand for structural and thermal applications, particularly in the aerospace and automotive industries [4,5]. Al-based MMCs offer a unique combination of properties, including the ductility of the matrix and the strength of the reinforcement, that cannot be found in conventional unreinforced materials [4,6]. Various materials comprised of ceramics (e.g., SiO_2, Al_2O_3, SiC, TiC, TiB_2, ZrB_2 and AlN), metallic glasses and complex metallic alloys have been successfully used as reinforcements in Al-based MMCs in the form of fibers, flakes or particulates [7–15]. Amongst them, particulate-reinforced MMCs are particularly attractive due to their easier fabrication routes and lower costs compared to fibers or flakes [4,13].

Metallic glasses have been recently proposed as an effective type of reinforcement due to their exceptional mechanical properties, such as high strength, hardness and corrosion resistance [16–18]. Metallic glasses are believed to be more compatible with the metal matrix and may lead to improved interface strength between the matrix and reinforcement than their ceramic counterparts [16–18]. In addition, the sintering process conducted within supercooled liquid (SCL), where metallic glasses display a significant decrease of viscosity, can assist with the consolidation, resulting in bulk samples with reduced porosity [18,19]. Thus, in order to obtain highly-dense materials with increased mechanical properties, Al-, Zr-, Fe-, Ni- and Cu-based metallic glass particles or ribbons have been used as reinforcements in Al-based metal matrix composites [17–24]. Amongst the different types of metallic glasses, Fe-based glasses are of considerable interest, because of their ultrahigh strength, good corrosion resistance, low cost, excellent soft magnetic properties, good glass forming ability and large SCL region [25–29]. Aljerf *et al.* reported that the use of $[(Fe_{1/2}Co_{1/2})_{75}B_{20}Si_5]_{96}Nb_4$ glassy particles as reinforcement in the Al-6061 alloy leads to a remarkable combination of high strength and plasticity [19]. Similar results have been recently reported for Al-2024 matrix composites reinforced with $Fe_{73}Nb_5Ge_2P_{10}C_6B_4$ glassy particles [30].

Powder metallurgy is one of the methods successfully used for the preparation of MMCs [1,7,31]. The main advantage of powder metallurgy over other techniques is the low processing temperature, which may prevent unwanted interfacial reactions between the matrix and reinforcement and which permits the economic feasibility of large-scale production, thus allowing the commercial processing of MMCs [32,33]. Furthermore, it provides a homogeneous distribution of the reinforcements within the matrix, and it enables a high degree of control over the product microstructure (volume fraction, size, shape, *etc.*), which is comparatively limited in the casting or diffusion welding routes [7,24]. The current studies related to the metallic glass-reinforced Al-based MMCs produced via powder metallurgy are mainly focused on the effect of the glassy particle content on the properties of the

composites [23–25]. On the other hand, the effect of microstructural modifications, such as particle shape and interparticle distance, induced by mechanical treatments, like ball milling, as well as the influence of the consolidation method on the properties of Al-based MMCs have received relatively little attention.

In this study, Al-based MMCs reinforced with Fe-based glassy particles have been produced via powder metallurgy and the effects of milling time (1, 10, 30 and 50 h) and the consolidation process (hot press or hot press followed by hot extrusion) on the microstructure and mechanical properties are investigated.

2. Experimental Section

2.1. Raw Materials

Glassy particles with a nominal composition of $Fe_{50.1}Co_{35.1}Nb_{7.7}B_{4.3}Si_{2.8}$ were produced by high-pressure N_2 gas atomization. The samples produced by this method are powders with sizes ranging from 38–112 μm. Al powders with a purity of 99.5% and an average particle size of 125 μm were used as the matrix material.

2.2. Mechanical Milling

Milling experiments on the powder mixtures comprised of pure Al and 40 vol% glassy particles were performed using a Retsch PM400 planetary ball mill (Retsch, Dusseldorf, Germany) equipped with hardened steel balls and vials and without any process control agents. The powders were milled at room temperature for 1, 10, 30 and 50 h using a ball-to-powder mass ratio (BPR) of 10:1 and at a milling speed of 150 rpm. Such a low milling speed was used only to have uniform dispersion of the reinforcement in the matrix, unlike conventional mechanical milling or alloying. Milling was carried out as a sequence of 15-min milling intervals interrupted by 15-min breaks to avoid a strong temperature rise during milling. All sample handling was carried out in a Braun MB 150B-G glove box under purified Ar atmosphere (less than 0.1 ppm O_2 and H_2O) in order to minimize atmospheric contamination.

2.3. Consolidation

Consolidation of the composite powders was done by uni-axial hot pressing (HP) or hot pressing followed by hot extrusion (HE) under Ar atmosphere at 673 K and 640 MPa. Hot pressing time and the hot extrusion ratio were 30 min and 4:1, respectively.

2.4. Characterization of the Powders and Consolidated Samples

Phase analysis of the powders and consolidated samples was performed by the X-ray diffraction technique (XRD) using a D3290 PANalytical X'pert PRO (PANalytical, Almelo, The Netherlands) with Co-Kα radiation ($\lambda = 0.17889$ nm) in the Bragg–Brentano configuration. After applying a series of metallographic treatments, microstructural characterization and elemental mapping of the consolidated samples were carried out by scanning electron microscopy (SEM, Zeiss, Oberkochen,

Germany) using a Gemini 1530 microscope (operated at 15 kV) equipped with energy-dispersive X-ray detection (EDX). The matrix ligament size ($\lambda = L/N$) was calculated from the arithmetic mean of ten measurements by superposing random lines on the high magnification SEM micrographs of the composites. It is determined by the total length falling in the matrix (L) and by counting the number of matrix region intercepts per unit length of test line (N). The thermal behavior of the powders was investigated by differential scanning calorimetry (DSC) with a Perkin-Elmer DSC7 calorimeter (Perkin Elmer, Waltham, MA, USA) at a heating rate of 20 K/min under a continuous flow of purified Ar.

The experimental densities of the consolidated samples were evaluated by the Archimedes principle, and the relative densities were calculated as the percent value from the ratio of the experimental to the theoretical density of Al matrix composite reinforced with 40 vol% $Fe_{50.1}Co_{35.1}Nb_{7.7}B_{4.3}Si_{2.8}$ (4.43 g/cm^3). Microhardness measurements were conducted by a computer-controlled Struers Duramin 5 Vickers hardness tester using a load of 10 g and indenter dwell time of 10 s. The microhardness test result of each sample includes the arithmetic mean of twenty successive indentations and standard deviations. Optical micrographs of the representative hardness indentations performed on the glassy phase distributed Al matrix were also given for each sample. Since the hardness comparison of the composites was aimed at a constant load, measurements were not directly applied on the glassy phase, whose indentation requires a higher value of load than the one utilized. Five different cylindrical specimens 2 mm diameter and 4 mm length were prepared from each of the hot pressed and hot extruded samples and tested at room temperature using an Instron 8562 testing facility under quasistatic compressive loading (strain rate 8×10^{-4} s^{-1}). Both ends of these specimens were carefully polished to make them parallel to each other prior to the compression tests. The strain during compression was measured directly on the specimens using a Fiedler laser-extensometer.

3. Results and Discussion

3.1. Processing and Characterization of the Composite Powders

Figure 1a–c illustrates the XRD patterns of the starting and composite powders milled for different times. Figure 1a shows the XRD patterns of the gas-atomized $Fe_{50.1}Co_{35.1}Nb_{7.7}B_{4.3}Si_{2.8}$ and pure Al (The International Centre for Diffraction Data (ICDD) Card No: 01-072-3440) powders. The glassy powder is not completely amorphous and shows the typical broad maxima characteristic for glassy materials at angles between $2\theta = 40°$ and $2\theta = 60°$ together with small diffraction peaks at about $2\theta = 41°$, 45°, 50° and 53°. As previously reported for gas-atomized Al-based glassy powders, the cooling rate may not be sufficient to completely suppress the formation of crystalline phases during gas atomization [34]. Figure 1b shows the XRD patterns of the composite powders with 40 vol% $Fe_{50.1}Co_{35.1}Nb_{7.7}B_{4.3}Si_{2.8}$ milled for 1, 10, 30 and 50 h, revealing sharp Bragg peaks, which correspond to the Al matrix. No peaks belonging to additional phases can be observed even after milling for 50 h. Moreover, the Al peaks are broadened, and their intensities gradually decrease with increasing milling time from 1–50 h, indicating a gradual decrease of the crystallite size, as well as the increase in the lattice strain. The weak and diffuse peak at about $2\theta = 50°–53°$ indicates the existence of the glassy phase in the Al matrix and proves the amorphous structure of the glassy phase after milling for 1 h. Further milling does not result in significant structural changes.
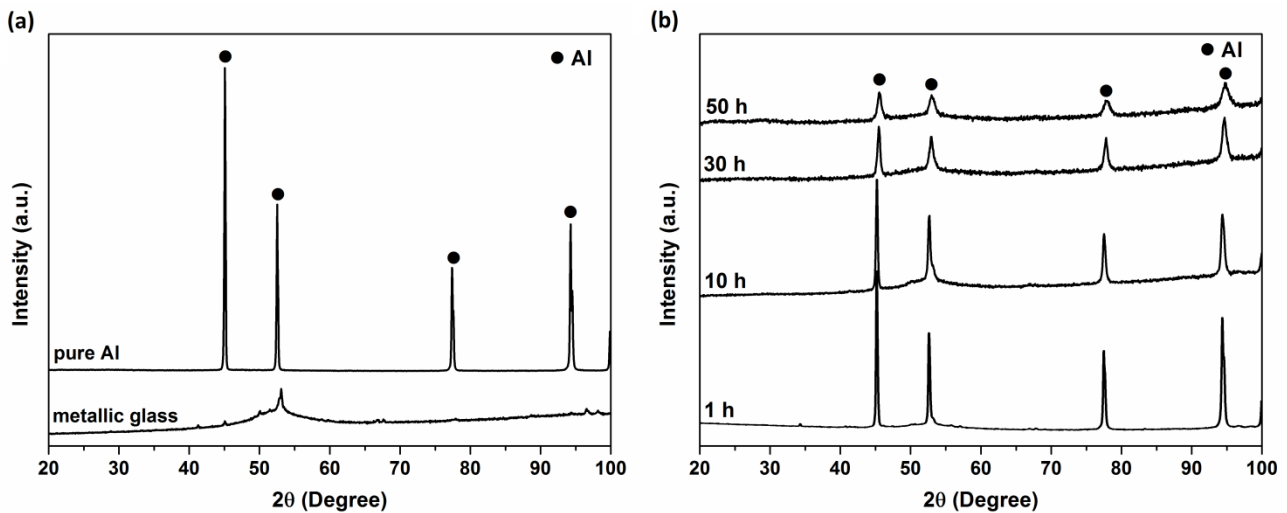
Figure 1. XRD patterns of the starting and composite powders milled for different times: (**a**) pure Al and metallic glass powders; and (**b**) composite powders milled for 1, 10, 30 and 50 h.

Figure 2a displays the DSC scan of the gas-atomized $Fe_{50.1}Co_{35.1}Nb_{7.7}B_{4.3}Si_{2.8}$ glassy powder. The scan displays a glass transition (T_g) at 838 K followed by a crystallization event with the onset (T_x) at 853 K. This is similar to what was observed for the $[(Fe_{1/2}Co_{1/2})_{75}B_{20}Si_5]_{96}Nb_4$ metallic glass, which has T_g and T_x values of 821 and 861 K, respectively [19]. DSC experiments were also carried out for the milled composite powders (Figure 2b) to analyze the effect of milling on T_g and T_x and to select the appropriate consolidation temperature. The DSC curves reveal a glass transition temperature (T_g) followed by the supercooled liquid (SCL) region (defined as $\Delta T_x = T_x - T_g$) before crystallization occurs at higher temperatures (T_x). The SCL regions lie below the melting temperature of the Al matrix, except for the powder milled for 1 h, which has T_x above 920 K. T_g values peaking with very weak endotherms are located at about 837, 800, 733 and 720 K, respectively, for the powders milled for 1, 10, 30 and 50 h. The prolonged milling time from 1–50 h results in a shift of T_g of about 117 K to lower temperatures. Continuous mechanical deformation of powder particles disturbs the bonds, creates dislocations, increases the fresh reactive surfaces of the particles and improves the chemical reactivity [32]. The shift of the glass transition temperature is larger (104 K) for the milling period between 1 and 30 h, whereas it is smaller for the powder milled between 30 and 50 h (13 K). Therefore, milling for 50 h is sufficient to get a desirable reduction in the T_g value of the composite powder, which correspondingly increases the temperature range of the SCL region. Figure 2b also displays broad exothermic events (corresponding to the crystallization of the glassy phase) with onset (T_x) at about 853, 840 and 837 K for the powders milled for 10, 30 and 50 h, therefore decreasing gradually with increasing the milling time. T_x determines the upper temperature limit for the sintering process, because at T_x, metallic glasses lose their liquid-like behavior, and the viscosity increases as crystallization starts [35].
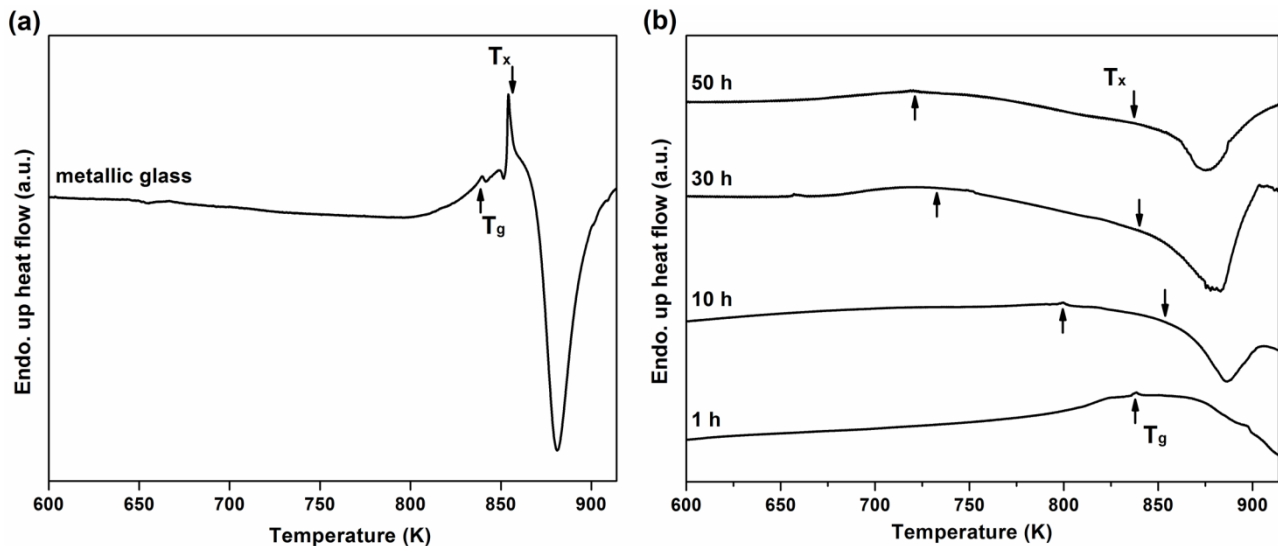
Figure 2. DSC scans (**a**) of the gas-atomized $Fe_{50.1}Co_{35.1}Nb_{7.7}B_{4.3}Si_{2.8}$ powder and (**b**) of the composite powders milled for 1, 10, 30 and 50 h.

The exothermic peaks in Figure 2b are rather broad, in contrast with what is generally observed for the crystallization of metallic glasses. This can be explained by the peak overlap for the peaks related to the crystallization of the glass and to the reaction of the Al matrix with the metallic glass induced by partial Al melting. When the crystallization temperature of the glassy phase in the composites is higher than that of Al melting, the corresponding DSC scan exhibits an endothermic event corresponding to the Al melting at about 835–897 K [21]. On the other hand, similar crystallization and Al melting temperatures were observed for Al-based composites reinforced with $Ni_{60}Nb_{40}$ metallic glass particles [18]. Similar to the present study, they showed broad exotherms in the DSC scans instead of the sharp peaks corresponding to the crystallization of the metallic glass [18]. The reason for this behavior was attributed to the amount of heat release originating from the $Ni_{60}Nb_{40}$ reinforcement, which was diluted in the Al matrix [18]. Furthermore, the reaction of the Al matrix with the metallic glass was observed, supported by the appearance of low-intensity diffraction peaks of aluminide intermetallics ($NiAl_3$ and $NbAl_3$) in the XRD patterns after annealing the composites at temperatures between 893 and 913 K [18].

3.2. Characterization of the Consolidated Samples

Figure 3a exhibits the XRD patterns of the hot pressed composites milled for different times. The patterns display the peaks of the Al matrix along with the diffuse amorphous halo at about $2\theta = 53°$. This indicates that, after consolidation, the glassy reinforcement remains amorphous, corroborating the DSC results showing the exothermic event due to crystallization of the glassy phase. Figure 3c shows the XRD patterns of the hot pressed and hot extruded composites milled for different times. The comparison of Figure 3a and Figure 3c reveals the effect of hot extrusion on the microstructure: after extrusion, the characteristic Al peaks become narrower, and their intensities increase with respect to the hot pressed samples, indicating an increase in the crystallite size, probably due to the stress-induced grain growth during secondary consolidation [36]. As seen in Figure 3c, a small amount of Al_5Fe_2 (ICDD Card No: 00-029-0043) is formed in the extruded specimens. The amount of the

Al_5Fe_2 phase increases with increasing the milling time, as expected from the contribution of deformation-induced crystallization.
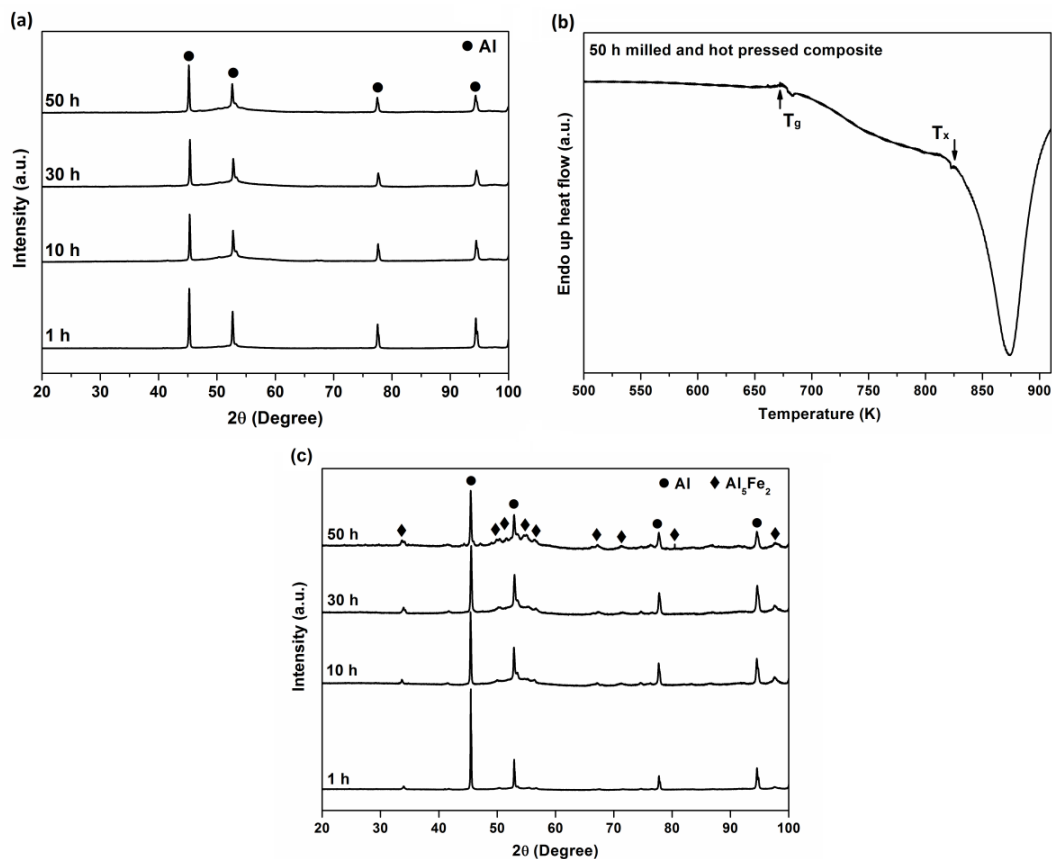

Figure 3. XRD patterns and DSC scan of the milled and consolidated samples: (**a**) XRD patterns of the hot pressed, (**b**) DSC scan of the 50-h milled and hot pressed and (**c**) XRD patterns of the hot pressed and hot extruded composites.

Figure 4a–d shows the SEM micrographs and the EDX elemental maps of the hot pressed composites. The SEM micrographs consist of dark and bright regions corresponding to the Al matrix and Fe-based glassy particles, as shown by the EDX analysis. The images also reveal the irregular shape and size of the Fe-based glassy particles embedded in the continuous Al matrix without observable cracks. The hot pressed composite produced from the powders milled for 1 h is characterized by a microstructure containing spherical glassy particles with an average size of 34 ± 8 μm and only a few pores (marked by arrows in Figure 4a). With increasing the milling time to 50 h (Figure 4d), repeated cold-welding, fracturing and re-welding [32] led to the formation of a heterogeneous microstructure consisting of large spheroidal particles along with small layered glassy particles. This gives rise to a smaller average size and to a broader particle size distribution (15 ± 12 μm). The decrease in the particle size of the Fe-based glassy particles resulting from the mechanically-induced fragmentation and the corresponding decrease of the inter-particle distance can be clearly seen in Figure 4a–d. The reduction of the distance between the particles can contribute considerably to the strength of the composites, because the matrix/particle interface can effectively inhibit dislocation movement [14].
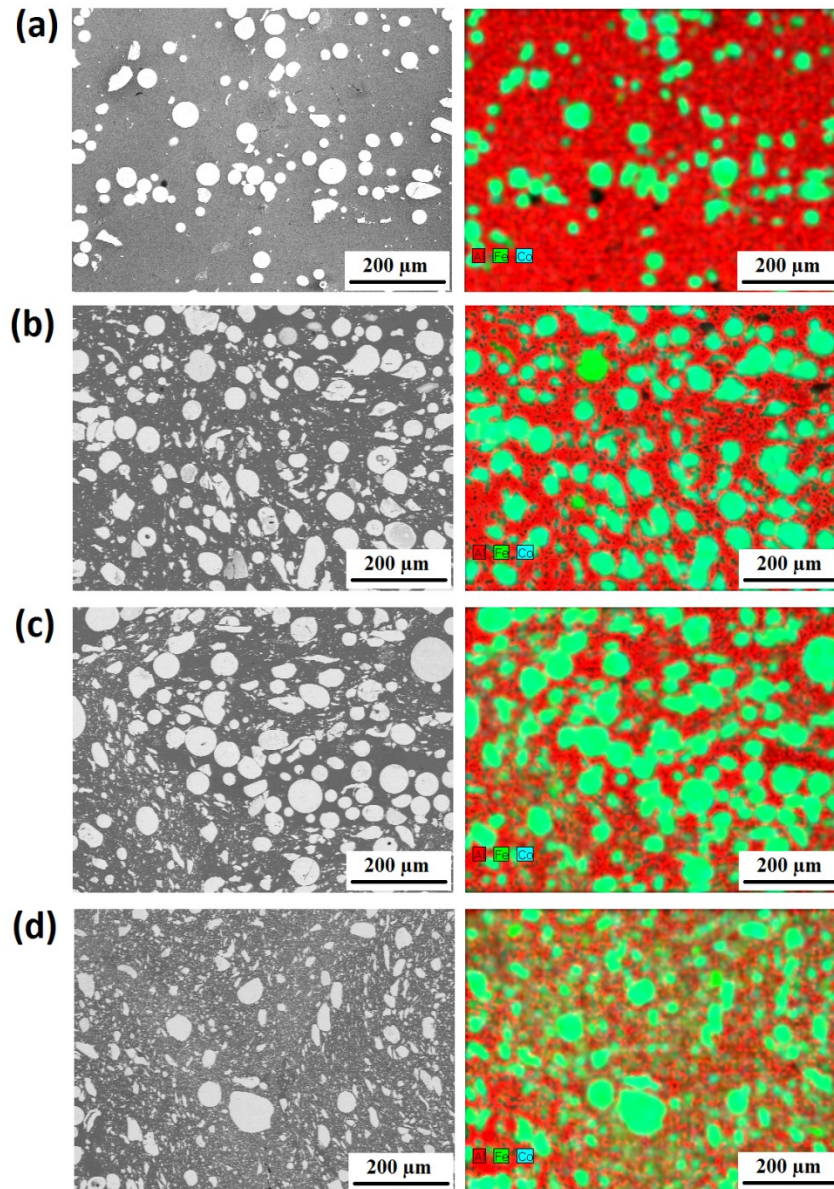
Figure 4. SEM micrographs and EDX maps of the hot pressed composites obtained from (**a**) 1-h, (**b**) 10-h, (**c**) 30-h and (**d**) 50-h milled powders.

Figure 5a–d illustrates the SEM micrographs of the hot extruded composites. The effects of milling on the microstructures of hot extruded samples are very similar to what was observed for the hot pressed samples. Compared to the hot pressed composites (Figure 4), hot extrusion leads to samples with enhanced density, as no pores are observed in the SEM micrographs (Figure 5). Although the XRD patterns in Figure 3c show the Al_5Fe_2 intermetallic product after hot extrusion, the matrix/particle interface of the hot extruded samples is clean, and no reaction zone is observed in Figure 5a–d. The Al_5Fe_2 phase cannot be detected by SEM, most likely because of the ultrafine dimension, as supported by the broad XRD peaks for this phase (Figure 3c). Furthermore, elongation of some large glassy particles occurs during hot extrusion with respect to the corresponding particles observed previously in the hot pressed composites (Figure 4a–d).
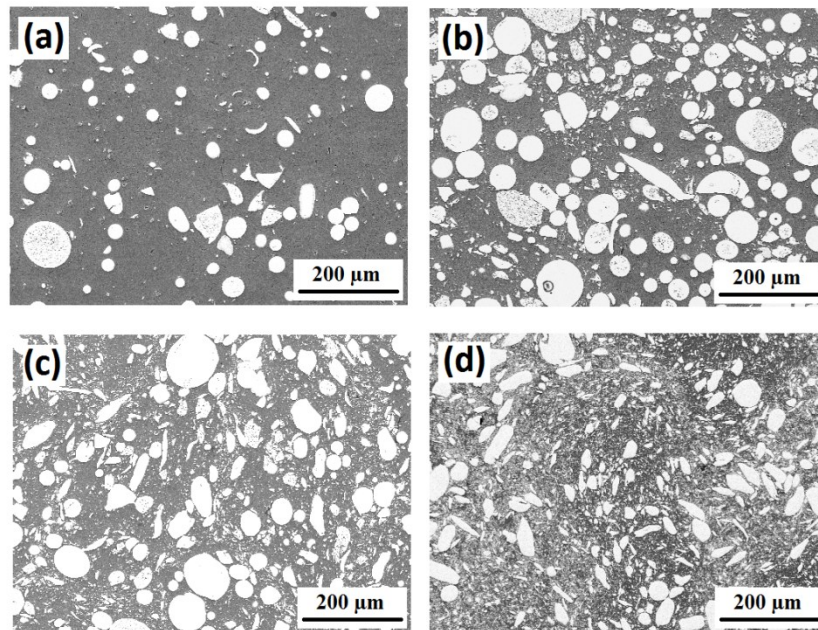
Figure 5. SEM micrographs of the hot pressed and hot extruded composites obtained from (**a**) 1-h, (**b**) 10-h, (**c**) 30-h and (**d**) 50-h milled powders.

The relative density (theoretical-experimental density) of the hot pressed and hot pressed and hot extruded composites are respectively ~98% and ~99%, as also supported by the SEM micrographs given in Figures 4 and 5, which show few or no pores. Therefore, hot pressing and hot extrusion provide nearly fully-dense specimens, since the combination of temperature and pressure stimulates the accelerated densification process and the elimination of residual porosity [37]. No significant effect of the milling time on the relative density of the composites is observed.

3.3. Mechanical Properties of the Consolidated Samples

Figure 6a,b displays the microhardness values of the composites as a function of milling time along with the optical micrographs of the indentations (under the same applied load). With increasing the milling time from 1–50 h, the microhardness increases from 51 ± 2.3–155 ± 6.5 HV for the hot pressed composites (Figure 6a) and from 45.1 ± 2.2–144 ± 10.5 HV for the hot pressed and hot extruded samples (Figure 6b). For a given milling time, the hardness of the hot pressed samples is higher than those of the hot pressed and hot extruded material. This can be explained by the smaller particle sizes (15 ± 12 μm) and more homogeneous distribution of the hard Fe-based glassy particles throughout the hot pressed microstructure than those consolidated by hot extrusion (22 ± 10 μm) [38]. A maximum average hardness value of 155 HV was measured for the 50-h milled and hot pressed sample, which is compatible with its microstructure, presenting a uniform distribution of fine glassy particles without significant clustering (Figure 4d). Moreover, the pyramidal indentations are not distorted, and no significant cracks are observed around the indentation, despite the difference in hardness between the soft matrix and the hard reinforcing phase (Figure 7). This indicates that the Fe-based glassy particles are strongly bonded with the Al matrix, which can play a significant role in enhancing the mechanical properties of the composites [30].
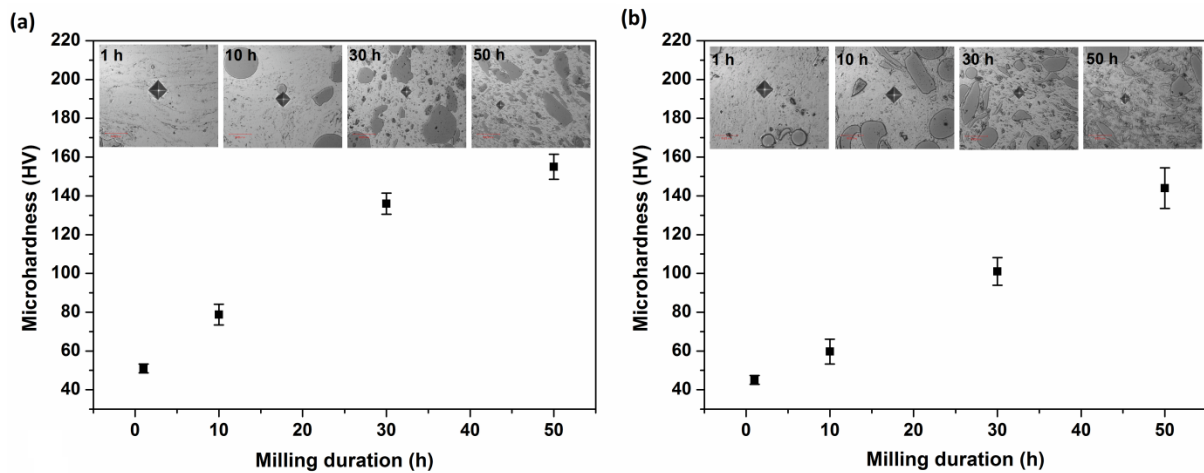
Figure 6. Microhardness values as a function of milling time and optical micrographs of the indentation marks obtained from: (**a**) hot pressed and (**b**) hot pressed and hot extruded composites.
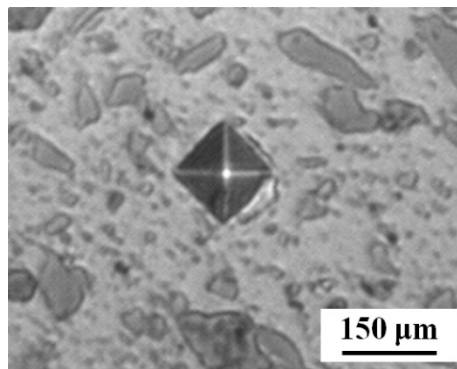

Figure 7. Optical microscopy image showing the indentation mark taken from the 50-h milled and hot pressed composite.

Room temperature compression true stress-true strain curves of the tests under quasistatic loading for the composite materials are shown in Figure 8. Data for the yield strength (0.2% offset), ultimate strength, strain at fracture and microhardness of the composites are summarized in Table 1. The yield and ultimate strength values of the composites are higher than those of the hot pressed and hot extruded pure Al (125 and 155 MPa, respectively), indicating the positive effect of Fe-based metallic glass reinforcements on the mechanical properties of Al [27,30]. These results also reveal the significant effect of milling and the consolidation process on the strength and plasticity of the composites. With increasing milling time from 1–50 h, the strength of the composites increases remarkably for both consolidation processes, showing a similar tendency as the hardness.

The ultimate strength of the hot pressed materials increases from 220 MPa for the composite milled for 1 h to 340, 440 and 630 MPa for the composites milled for 10, 30 and 50 h, respectively. In contrast, the plastic deformation of the hot pressed materials decreases from 35% for the composite milled for 1 h to 8.5%, 6.5% and 1.2% for the hot pressed composites produced from the powders milled for 10, 30 and 50 h. On the other hand, the ultimate strength of the hot extruded materials increases from 220 MPa for the composite milled for 1 h to 295 MPa for the composites milled for

10 h, while retaining appreciable plastic deformation, reaching an ultimate strain of 30% before fracture occurs. The 30 h milled, hot pressed and hot extruded composite gives a good combination of high strength and remarkable plasticity, exhibiting yield and ultimate strengths at 285 and 390 MPa and fracture strain at 21%.
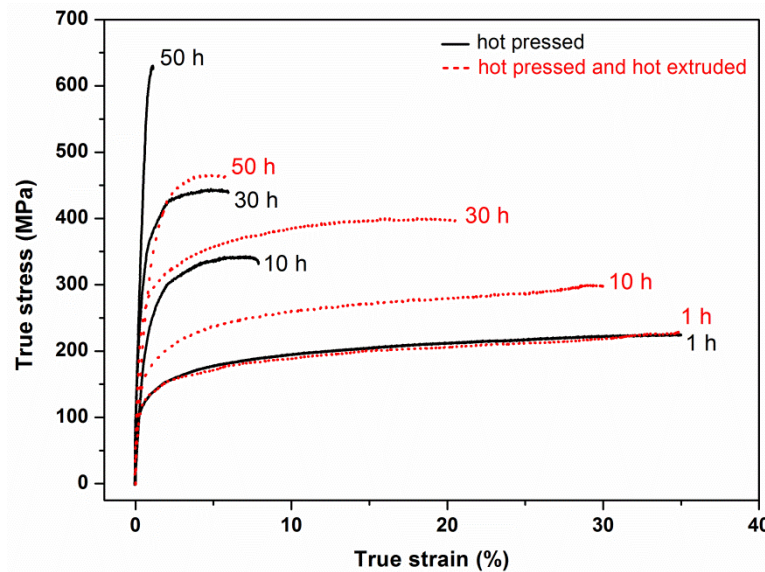

Figure 8. Room temperature compression true stress-true strain curves of the consolidated samples obtained from 1-, 10-, 30- and 50-h milled powders: (━) hot pressed and (━) hot pressed and hot extruded composites.

Table 1. Mechanical properties of Al metal matrix composites (MMCs) reinforced with 40 vol% $Fe_{50.1}Co_{35.1}Nb_{7.7}B_{4.3}Si_{2.8}$ metallic glass particles produced by mechanical milling for different times, hot pressing (HP) and hot pressing followed by hot extrusion (HP + HE) at 673 K and 640 MPa, as derived from the uniaxial compression and Vickers microhardness tests.

Milling time (h)	Consolidation process	Yield Strength (MPa)	Ultimate Strength (MPa)	Strain at Fracture (%)	Vickers Microhardness (HV)
1	HP	125	220	35.0	51 ± 2
	HP + HE	125	220	35.0	45 ±2
10	HP	275	340	8.5	79 ± 5
	HP + HE	180	295	30.5	60 ± 6
30	HP	350	440	6.5	136 ± 5
	HP + HE	285	390	21.0	101 ± 7
50	HP	595	630	1.2	155 ± 7
	HP + HE	340	470	6.5	144 ± 11

These results show that the use of hot extrusion after hot pressing slightly reduces both the strength and hardness of the composites, while raising the plastic deformation, which ranges between 35 and 6.5%. The values of strength for the 50-h milled and consolidated samples are higher than those reported for Al/Al₂O₃ composites [39] and Al MMCs reinforced with different types of metallic

glasses [21,25]. This indicates that Fe-based glassy particles may be a valid alternative to the conventional ceramic or other metallic glass reinforcements.

As revealed by the XRD patterns and SEM micrographs of the powders and consolidated samples (Figures 1 and 3–5), milling leads to the reduction of the reinforcement particle size (Figure 9), which is most likely the reason for the increase of the yield and ultimate strengths with increasing milling time (Table 2). The reduction of the particle size leads to an improvement in the mechanical properties if a clean particle-matrix interface is obtained [4]. The average inter-particle distance of the composites decreases to 3 μm after milling for 50 h. This observation can be translated into an effective grain size of the Al matrix in the composites smaller than 3.5 μm [30]. Besides the reduced particle size, the improvement of the strength and hardness of the composites resulting from milling can also be ascribed to the corresponding reduced distance between the glassy particles, as observed in the SEM micrographs (Figures 4 and 5). This phenomenon was reported for the Al and brass matrix composites reinforced with different types of metallic glasses [18,35].

Table 2. The average inter-particle distance for the hot pressed and hot pressed and hot extruded composites as a function of milling time.

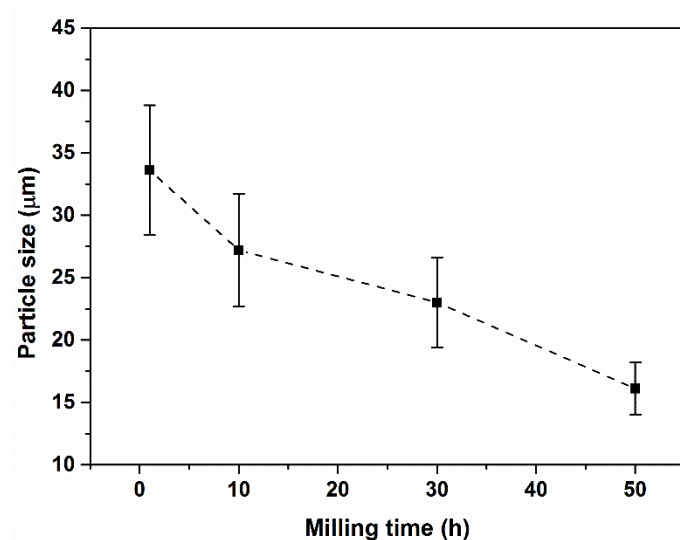| Milling Time (h)	Average inter-particle distance (μm)	
	Hot pressed composites	Hot pressed and hot extruded composites
1	21 ± 7	26 ± 7
10	8 ± 1	10 ± 2
30	6 ± 2	6 ± 1
50	3 ± 1	4 ± 1

Figure 9. Average particle sizes of the hot pressed composites milled for different times.

3.4. Evaluation of the Mechanical Behavior by Theoretical Predictions

The prediction of the mechanical properties of a composite is an important prerequisite for material design and application. Recently, a model proposed by Gurland [40], which considers ($\sigma \propto V^{1/3}d^{-1/2}$)

the combined effects of the reinforcement volume fraction (*V*) and the particle size (*d*), has been rearranged to consider the effect of the matrix ligament size λ, as [35]:

$$\sigma \propto V^{1/3} \lambda^{-1/2} \tag{1}$$

Figure 10a,b shows the yield strength as a function of $V^{1/3}\lambda^{-1/2}$ for the present consolidated samples. The matrix ligament size depends on the milling time of the composite powders, and for the current volume fraction of reinforcement (40 vol%), the relationship between strength and $V^{1/3}\lambda^{-1/2}$ is linear for both hot pressed and hot extruded samples. The reduction of *λ* can give a considerable contribution to the strength of the composites because the matrix/particle interface can effectively reduce the movement of dislocations [15]. This corroborates the validity of the model (Equation (1)) for the present composites and further indicates that the strength can be accurately modeled by considering the effect of the matrix ligament size. Furthermore, the reason for the differences in strength and plasticity of the hot pressed and hot extruded composites can be explained by the grain growth of the Al matrix and the formation of particle clusters during hot extrusion, as previously observed in Figures 3c and 5. The grain refinement provides an additional strengthening effect resulting from the dislocation piling-up at the grain boundaries [41–43].
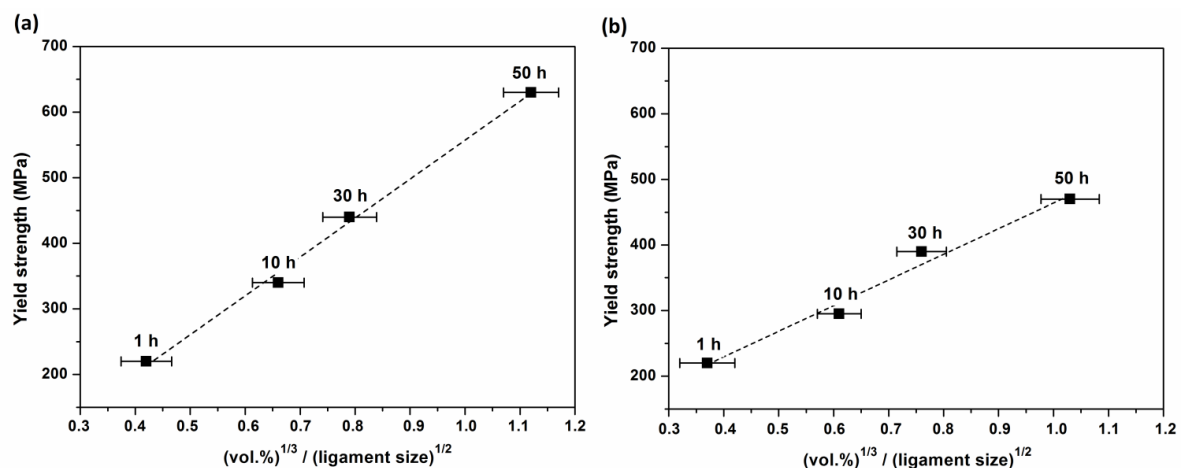

Figure 10. Yield strength as a function of volume fraction and matrix ligament size ($\sigma \propto V^{1/3} \lambda^{-1/2}$) for consolidated samples: (**a**) milled and hot pressed and (**b**) milled, hot pressed and hot extruded composites.

Eventually, composites fabricated by milling for different times, hot pressing and hot extrusion can be considered as potential candidates for applications demanding various mechanical properties. The hot pressed composites exhibit high strength and high hardness, which are of primary importance for structural applications [1]. On the other hand, hot extruded MMCs are potential materials for aerospace and automotive industries due to a superior balance of improved strength and plasticity [1].

4. Conclusions

Al matrix composites reinforced with 40 vol% $Fe_{50.1}Co_{35.1}Nb_{7.7}B_{4.3}Si_{2.8}$ glassy particles have been successfully produced via powder metallurgy routes using different milling times and consolidation processes. Based on the results of the present study, the following conclusions can be drawn:

1. Milled and hot pressed composites revealed no formation of intermetallic compounds even after milling for 50 h, within the sensitivity of the XRD measurements. Only a small amount of the Al_5Fe_2 intermetallic compound was observed in the XRD patterns of all milled, hot pressed and hot extruded samples. DSC scans revealed that milling time changes the overall crystallization behavior of the composite powders.

2. Ball milling resulted in the decrease of the grain sizes of the Al matrix, in the reduction of the particle size of the glassy reinforcements and in their homogeneous distribution in the Al matrix. This has a positive effect on the hardness and strength of the composites produced by both hot pressing and hot pressing followed by hot extrusion. With increasing the milling time from 1−50 h, the microhardness values of the hot pressed and hot extruded samples increase from 51 ± 2.26–155 ± 6.5 HV and from 45.1 ± 2.24–144 ± 10.5 HV, respectively. With increasing milling time from 1−50 h, the strength of the composites increases remarkably for both consolidation processes, showing a similar tendency as observed for the hardness.

3. The ultimate strength of the hot pressed materials increases from 220 MPa for the composite milled for 1 h to 340, 440 and 630 MPa for the composites milled for 10, 30 and 50 h, respectively. The 50-h milled and hot pressed composite exhibits small plastic deformation of 1.2% and a maximum strength of 630 MPa, which is in agreement with the highest Vickers microhardness of 155 ± 6.5 HV among all composites.

4. The use of hot extrusion after hot pressing slightly reduces both the strength and hardness of the composites, while raising the plastic deformation ranging between 35 and 6.5%. The 30-h milled, hot pressed and hot extruded composite gives a combination of high strength (390 MPa) and remarkable plasticity (21%).

The strength of both the hot pressed or hot pressed and hot extruded composites can be accurately described by a simple model considering the effect of matrix ligament size on the strengthening of the composites.

Acknowledgments

Author Contributions

Özge Balcı performed all the experiments and characterization studies and created the initial draft. Konda Gokuldoss Prashanth aided in SEM analyses and mechanical tests and conceived the final manuscript. Sergio Scudino formulated the idea of this research, designed the experiments and supervised the discussion of the results. Duygu Ağaoğulları, İsmail Duman and M. Lütfi Öveçoğlu aided the review of the paper and provided critical comments. Volker Uhlenwinkel prepared the gas-atomized glassy powders used in the experiments. Jürgen Eckert contributed to the overall development of the main concepts of this study.

Conflicts of Interest

The authors declare no conflict of interest.

References

1. Epple, M. *Biomaterialien und Biomineralisation—Eine Einführung für Naturwissenschaftler, Mediziner und Ingenieure*; Springer: Wiesbaden, Germany, 2003.
2. Miracle, D.B. Metal matrix composites—From science to technological significance. *Compos. Sci. Technol.* **2005**, *65*, 2526–2540.
3. Miracle, D.B.; Donaldson, S.L. Composites. In *ASM Handbook*; ASM International: Materials Park, OH, USA, 2001.
4. Davis, J.R. Aluminum and Aluminum alloys. In *ASM Specialty Handbook*; ASM International: Materials Park, OH, USA, 1993.
5. Clyne, T.W.; Withers, P.J. *An Introduction to Metal Matrix Composites*; Cambridge University Press: New York, NY, USA, 1993.
6. Kainer, K.U. *Metal Matrix Composites: Custom-Made Materials for Automotive and Aerospace Engineering*; WILEY-VCH: Weinheim, Germany, 2006.
7. Christman, T.; Needleman, A.; Suresh, S. An experimental and numerical study of deformation in metal-ceramic composites. *Acta Metall.* **1998**, *37*, 3029–3050.
8. Slipenyuk, A.; Kuprin, V.; Milman, Y.; Goncharuk, V.; Eckert, J. Properties of P/M processed particle reinforced metal matrix composites specified by reinforcement concentration and matrix-to-reinforcement particle size ration. *Acta Mater.* **2006**, *54*, 157–166.
9. Song, M.S.; Zhang, M.X.; Zhang, S.G.; Huang, B.; Li, L.G. *In situ* fabrication of TiC particulates locally reinforced aluminum matrix composites by self-propagating reaction during casting. *Mater. Sci. Eng. A* **2008**, *473*, 166–171.
10. Wang, J.; Yi, D.; Su, X.; Yin, F.; Li, H. Properties of submicron AlN particulate reinforced aluminium matrix composite. *Mater. Des.* **2009**, *30*, 78–81.
11. Feng, C.F.; Froyen, L. *In situ* synthesis of Al_2O_3 and TiB_2 particulate mixture reinforced aluminium matrix composites. *Scr. Mater.* **1997**, *36*, 467–473.
12. Arsenault, R.J. The strengthening of aluminum 6061 by fiber and platelet silicon carbide. *Mater. Sci. Eng. A* **1984**, *64*, 171–181.
13. Balcı, Ö.; Ağaoğulları, D.; Gökçe, H.; Duman, İ.; Öveçoğlu, M.L. Influence of TiB_2 particle size on the microstructure and properties of Al matrix composites prepared via mechanical alloying and pressureless sintering. *J. Alloys Compd.* **2013**, *586*, S78–S84.
14. Ibrahim, I.A.; Mohammed, F.A.; Lavernia, E.J. Particulate reinforce metal matrix composites: Review. *J. Mater. Sci.* **1991**, *26*, 1137–1156.
15. Scudino, S.; Liu, G.; Sakaliyska, M.; Surreddi, K.B.; Eckert, J. Powder metallurgy of Al-based metal matrix composites reinforced with β-Al_3Mg_2 intermetallic particles: Analysis and modeling of mechanical properties. *Acta Mater.* **2009**, *57*, 4529–4538.
16. Inoue, A. Bulk amorphous and nanocrystalline alloys with high functional properties. *Mater. Sci. Eng. A* **2001**, *304–306*, 1–10.

17. Ashby, M.F.; Greer, A.L. Metallic glasses as structural materials. *Scr. Mater.* **2006**, *54*, 321–326.

18. Yu, P.; Zhang, L.C.; Zhang, W.Y.; Das, J.; Kim, K.B.; Eckert, J. Interfacial reaction during the fabrication of $Ni_{60}Nb_{40}$ metallic glass particles-reinforced Al based MMCs. *Mater. Sci. Eng. A* **2007**, *444*, 206–213.

19. Aljerf, M.; Georgarakis, K.; Louzguine-Luzgin, D.; le Moulec, A.; Inoue, A.; Yavari, A.R. Strong and light metal matrix composites with metallic glass particulate reinforcement. *Mater. Sci. Eng. A* **2012**, *532*, 325–330.

20. Dudina, D.V.; Georgarakis, K.; Aljerf, M.; Li, Y.; Braccini, M.; Yavari, A.R.; Inoue, A. Cu-based metallic glass particle additions to significantly improve overall compressive properties of an Al alloy. *Compos. A* **2010**, *41*, 1551–1557.

21. Lee, M.H.; Kim, J.H.; Park, J.S.; Kim, J.C.; Kim, W.T.; Kim, W.T.; Kim, D.H. Fabrication of Ni–Nb–Ta metallic glass reinforced Al-based alloy matrix composites by infiltration casting process. *Scr. Mater.* **2004**, *50*, 1367–1371.

22. Yu, P.; Kim, K.B.; Das, J.; Baier, F.; Xu, W.; Eckert, J. Fabrication and mechanical properties of Ni–Nb metallic glass particle-reinforced Al-based metal matrix composite. *Scr. Mater.* **2006**, *54*, 1445–1450.

23. Scudino, S.; Surreddi, K.B.; Sager, S.; Sakaliyska, M.; Kim, J.S.; Löser, W.; Eckert, J. Production and mechanical properties of metallic glass-reinforced Al-based metal matrix composites. *J. Mater. Sci.* **2008**, *43*, 4518–4526.

24. Scudino, S.; Liu, G.; Prashanth, K.G.; Bartusch, B.; Surredi, K.B.; Murty, B.S.; Eckert, J. Mechanical properties of Al-based metal matrix composites reinforced with Zr-based glassy particles produced by powder metallurgy. *Acta Mater.* **2009**, *57*, 2029–2039.

25. Prashanth, K.G.; Kumar, S.; Scudino, S.; Murty, B.S.; Eckert, J. Fabrication and response of $Al_{70}Y_{16}Ni_{10}Co_4$ glass reinforced metal matrix composites. *Mater. Manuf. Processes* **2011**, *26*, 1242–1247.

26. Shen, T.D.; Schwarz, R.B. Bulk ferromagnetic glasses prepared by flux melting and water quenching. *Appl. Phys. Lett.* **1999**, *75*, 49–51.

27. Fujii, H.; Sun, Y.; Inada, K.; Ji, Y.; Yokoyama, Y.; Kimura, H.; Inoue, A. Fabrication of Fe-based metallic glass particle reinforced Al-based composite materials by Friction Stir processing. *Mater. Trans.* **2011**, *52*, 1634–1640.

28. Suryanarayana, C.; Inoue, A. Iron-based bulk metallic glasses. *Int. Mater. Rev.* **2013**, *58*, 131–166.

29. Kaban, I.; Jovari, P.; Waske, A.; Stoica, M.; Bednarcik, J.; Beuneu, B.; Mattern, N.; Eckert, J. Atomic structure and magnetic properties of Fe–Nb–B metallic glasses. *J. Alloys Compd.* **2014**, *586*, S189–S193.

30. Zheng, R.; Yang, H.; Liu, T.; Ameyama, K.; Ma, C. Microstructure and mechanical properties of aluminum alloy matrix composites reinforced with Fe-based metallic glass particles. *Mater. Des.* **2014**, *53*, 512–518.

31. Murty, B.S.; Ranganathan, S. Novel materials synthesis by mechanical alloying/milling. *Int. Mater. Rev.* **1998**, *43*, 101–141.

32. Suryanarayana, C. Mechanical alloying and milling. *Prog. Mater. Sci.* **2001**, *46*, 1–184.

33. Harrigan, W.C., Jr. Commercial processing of metal matrix composites. *Mater. Sci. Eng. A* **1998**, *244*, 75–79.

34. Surreddi, K.B.; Scudino, S.; Sakaliyska, M.; Prashanth, K.G.; Sordelet, D.J.; Eckert, J. Crystallization behavior and consolidation of gas-atomized $Al_{84}Gd_6Ni_7Co_3$ glassy powder. *J. Alloys Compd.* **2010**, *491*, 137–142.

35. Kim, J.Y.; Scudino, S.; Kühn, U.; Kim, B.S.; Lee, M.H.; Eckert, J. Production and characterization of Brass-matrix composites reinforced with $Ni_{59}Zr_{20}Ti_{16}Si_2Sn_3$ glassy particles. *Metals* **2012**, *2*, 79–94.

36. German, R.M. *Sintering Theory and Practice*; Wiley-Interscience: Weinheim, Germany, 1996.

37. Prashanth, K.G.; Murty, B.S. Production, kinetic study and properties of Fe-based glass and its composites. *Mat. Manuf. Processes* **2010**, *25*, 592–597.

38. Keryvin, V.; Hoang, V.H.; Shen, J. Hardness, toughness, brittleness and cracking systems in an iron-based bulk metallic glass by indentation. *Intermetallics* **2009**, *17*, 211–217.

39. San Marchi, C.; Cao, F.; Kouzeli, M.; Mortensen, A. Quasistatic and dynamic compression of aluminum-oxide particle reinforced pure aluminum. *Mater. Sci. Eng. A* **2002**, *337*, 202–211.

40. Gurland, J. The fracture strength of sintered tungsten carbide-cobalt alloys in relation to composition and particle spacing. *Trans. Metall. Soc. AMIE* **1963**, *227*, 1146–1149.

41. Chawla, K.K. *Composite Materials: Science and Engineering*; Springer-Verlag: New York, NY, USA, 1987.

42. Kim, H.S. On the rule of mixtures for the hardness of particle reinforced composites. *Mater. Sci. Eng. A* **2000**, *289*, 30–33.

43. Hirth, J.P. *Physical Metallurgy*, Cahn, R.W., Haasen, P., Eds.; North-Holland: Amstdam, The Netherlands, 1996.